Indonesian Journal of Electrical Engineering and Computer Science
Vol. 17, No. 3, March 2020, pp. 1362~1370
ISSN: 2502-4752, DOI: 10.11591/ijeecs.v17.i3.pp1362-1370

Veins projection performance based on ultrasonic distance sensor in various surface objects

I Putu Adi Surya Gunawan, Riyanto Sigit, Agus Indra Gunawan
Department of Electrical Engineering, Politeknik Elektronika Negeri Surabaya, Indonesia

Article Info

Article history:

Received Jun 10, 2019
Revised Sep 1, 2019
Accepted Oct 6, 2019

Keywords:

Back-projection
Intravenous therapy
Ultrasonic distance
Vein visualization

ABSTRACT

Intravenous therapy aims to inject fluids such as medicine or nutritions into the body via vein vessel. This procedure is needed in various cases whether in an ordinary or emergency. Every person has a different difficulty level thus a nurse usually encountered a problem when locating the position of vein vessel. A visualization device that able to work in realtime and have high mobility is really necessary for an emergency situation to speed up the intravenous access. In this study, a stand-alone veins visualization system was developed. The back-projection method that can adjust based on distance was used to speed up the visualization process. The distance between the device and the object is obtained by an ultrasonic distance sensor. The results of this projection method with a flat surface have maximum shift of 0.48 mm. While on various surfaces, projection shifts under 0.9 mm reach 89% from 140 measurement points. Projection shifts that reach more than 0.9 mm occurred due to the sensor readings are on steep curvature or large angles between segments and sensors.

Corresponding Author:

I Putu Adi Surya Gunawan,
Depatment of Electrical Engineering,
Politeknik Elektronika Negeri Surabaya, Indonesia.
Email: iputuadisurya@pasca.student.pens.ac.id

1. INTRODUCTION

The fastest way to deliver medications and fluid replacement throughout the body is via the intravenous route. Intravenous therapy may be used for fluid replacement (such as correcting dehydration), to deliver medications, to correct electrolyte imbalances, and for blood transfusions. In determining the location of veins, a nurse usually encounters problems because each person has a different level of difficulty. A flexible and real-time system will greatly assist a nurse in accelerating the visualization process. Currently there are tools to visualize veins such as AccuVein, VeinViewer, Vein Site but the price is still quite expensive [1].

Research on vein visualization is generally divided into 2 scopes: for security purposes and medical purposes. In medical purposes, research on vein visualization is more aimed at realtime visualization. Juric et al develope a vein visualization system using an android tablet as a platform to perform vein image processing and visualization in real-time [1]. Similar visualization technique also developed by Al Gozhali et al. on the PC platform [2]. The use of additional screen as a visualization media in those researches is considered unsuitable because nurses must look at the screen to observe the veins. Therefore, several studies have discussed the veins visualization system which is focused on applying visualization with direct projections on the patient's skin. Marcotti et al [3] was discussed about developement of veins visualization system. In his research, the position of the projector was placed far above the camera to get the correct projection. This back-projection method needs a large space and there was a limitation in projection distance that allow the user must performing visualization specific distance. Another method to visualize veins image was conducted by using a dual camera system to find the depth of a vein [4]. In this research, the distance

between objects and acquisition devices has been set at 35 cm. As seen from the projection method, there will be a shift in projection if the distance of the object does not match the distance that has been set. With a dual camera system, it is possible to know the distance between the device and the object and make adjustments to the projection at each distance. However, in his research only focused on a certain distance and the system requires very long computation time even though the image processing process is done on computers with processors running at 2.6 GHz. Meanwhile, a realtime and stand-alone system for vein visualization equipment will make it easier to use.

From previous studies, it is known that there are still problems related to the computational time and mobility of the developed visualization system. Therefore, this study proposes a real-time vein visualization system with high mobility in order to make it easier to use by a nurse. All computational processes are carried out using a single board computer. For a portable system, the use of a single camera and mini projector system was enough to perform the back-projection at a fixed point. However, just one point will be difficult to find and will slow down the intravenous process, thus this system must be able to perform back-projection correctly at a certain range of distances. Inspired by previous research [5], a concept of the back-projection method by adding a distance parameter to adjust the back-projection is worthy of further investigation. Regarding the results of research on distance measurement with ultrasonic sensors [6, 7], an idea to apply ultrasonic sensors on this system is desriable. In general, research on distance measurement with ultrasonic sensors is used in flat material [7, 8] while human skin has various surface shapes. Therefore, the process of testing the back-projection method will be carried out using objects with various surfaces in this study.

2. VEIN SPECTRUM ABSORBTION

Veins are blood vessels used for intravenous therapy. Blood in these vessels contains Deoxy Hb, while blood in arteries contains Oxy Hb. Based on the results of research on the absorption of the light spectrum that shown in Figure 1(a), it can be seen that veins and arteries have significant differences in absorption at wavelengths of around 680 nm [9]. On the other hand, there is a study developed by Travelakiz [10] to determine the absorption of the light spectrum in several paint samples shown in Figure 1(b). If observed at a wavelength of around 680 nm, it can be seen that Ultramarine Blue, Azurite, and Chromium Green have properties similar to Deoxy Hb. Whereas Vermilion, Cadmium Red, Chrome Yellow, and Zinc White have properties similar to Oxy Hb.

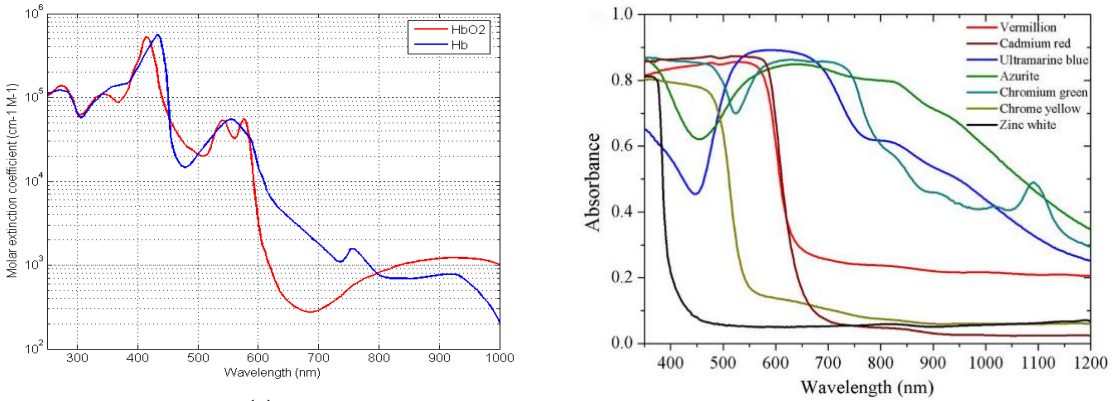

(a) (b)

Figure 1. (a) NIR spectrum absorption between Hb and HbO2 [9]; (b) NIR spectrum arbsorption in many samples paint [10]

3. RESEARCH METHOD

This study focused on development of real-time veins visualization with high mobility and flexibility. In order to achieve the high flexibility, back-projection concept that discussed in previous research [5] was necessary to implemented in this system. In this method, the distance is obtained by the ultrasonic sensor has an important role for determining the projection location. The distance is obtained by measuring time of flight of sound waves multiplied by sound wave velocity at the air [11]. However, this measurement

concept does not always get accurate results because the surface of the skin is not always flat. Therefore, several simulation objects with different surfaces as shown in

Figure 2 are used to test the performance of the back-projection method. These objects were made by acrylic material to create the shape. Simulated veins created by blue lines according to Figure 1(b) where the blue color will absorb infrared light as same as deoxyhemoglobin. This blue line was printed on a sketch paper and placed on the surface of the shape.

Figure 3(a) shows the system design in this study. The camera and ultrasonic distance sensor were used as input from this system. The frame produced by the camera was processed the microprocessor (Raspberry Pi 3B). The stages of image processing in this system consist of preprocessing, segmentation, and back-projection. The difference between veins and skin were strengthened in the preprocessing stage. The vein pattern was separated from the skin in the segmentation process before it projected in the back-projection stage. A mini projector was used as the output of this system to perform the back-projection method.

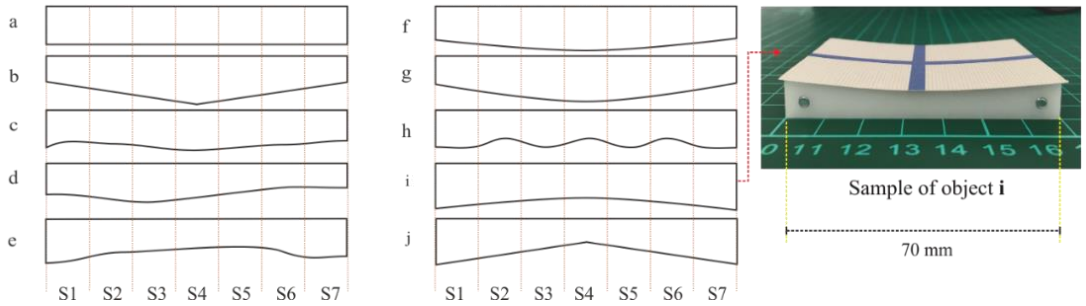

Figure 2. Objects with different surface

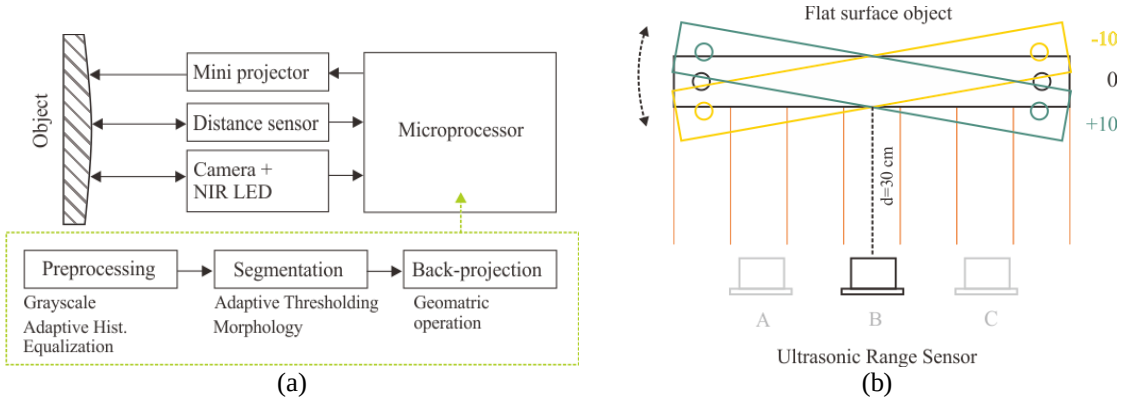

Figure 3. (a) System design; (b) Measurement setup to test the ultrasonic sensor

3.1. Vein Image Acquisition

The NoIR camera is a camera without an IR cut filter where the camera is able to see a near-infrared light spectrum (650-900) nm. When NIR light transmitted on the skin, it was scattered [12]. Some lights are reflected and some are forwarded inside due to the scaterization effect. Based on the results shown in Figure 1(a), the light that can be passed into the veins (near infrared ray) will be absorbed. The absorption process will cause dark colors in veins when observed with a NoIR camera. Therefore, the use of NIR spectrum [13, 14] has important role to obtain the vein pattern.

3.2. Preprocessing

The difference between the veins and the skin produced by the camera does not look so clear to identify. Therefore, the difference between veins and skin needs to be strengthened. Note that the frame obtained by the camera has an RGB format. However, the application of visible light block filters causes the captured frame only contain gray levels. Since the next process requires a grayscale image, the RGB type

image is reduced to 1 layer (grayscale). Some low-pass filter [15, 16] was performed to handle the noisy image.

Veins have a dark color because they absorb the NIR light given while the skin has a bright color. The contrast stretch process such as high-boost filter [17] or histogram equalization [18, 19] is widely used to reinforce the difference between veins and skin. Histogram equalization performs the calculation process obtained from all pixels in an image. Due to the distribution of vein patterns in an image is not uniform, the application of histogram equalization is less suitable because it can eliminate some information from vein images. Therefore, the use of adaptive histograms [19] or local histogram is more appropriate to use in this system.

3.3. Segmentation

The segmentation process aims to separate the vein pattern from the skin. The easiest segmentation method to do for a grayscale image is thresholding. However, general thresholding will affect each pixel in an image and allow lost information [20]. Therefore, the use of adaptive thresholding such as Niblack [21- 23] and Otsu [24] is expected to be able to overcome the lost information. Meanwhile, the threshold value for each block in this study is determined by the mean value of neighbors pixels minus center since the result give a good result and fast computation.

3.4. Back-projection

Vein image that already segmented will back-projected to the observation area. Based on the method used in this study shown in **Error! Reference source not found.**(a), a projection shift will be occurred if there is a change in distance between device and object. Therefore, a distance sensor is used as the main parameter to adjust the projection location. After the image processing is complete, the processed frame will be projected by determining the projection location (x,y) based on the distance between device and object.

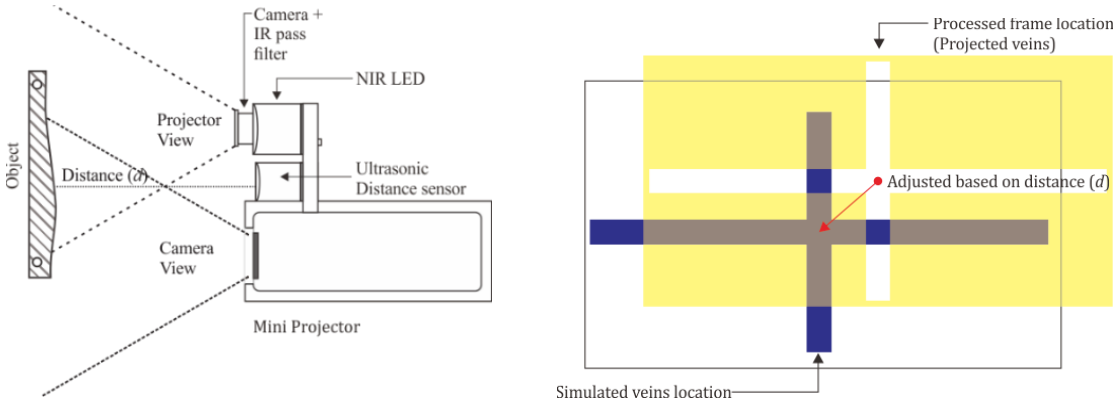

Figure 4. (a) Back-projection method; (b) adjustment of processed frame to the original object location

The projection location has been calibrated based on distance and a flat object which is expressed in (**Error! Reference source not found.**) and (**Error! Reference source not found.**). The processed frame was adjusted to original location area in the measured object as shown in **Error! Reference source not found.**(b). x and y are the location of processed frame in a full screen projector view with size of 1024*768 pixels.

$$x = 0.1294d^2 - 12.631d + 751.8 \quad (1)$$

$$y = -0.2775d^2 - 25.072d + 494.78 \quad (2)$$

Since the skin does not have a fairly flat surface, it is necessary to observe the performance of back-projections on objects with different surfaceses as shown in

Figure 2. All objects have the same length of 70 mm and were divided into several segments i.e. S1, S2, …, S7 as shown in Figure 4(a). The mechanism of measurement and placement of sensor against

object is shown in Figure 4(b). Sensor position is perpendicular to the object base and fixed. The distance between sensor and base of the object is 30 cm. Meanwhile, the ultrasonic sensor can move verticaly in order to measure distance (d) from S1 to S7.

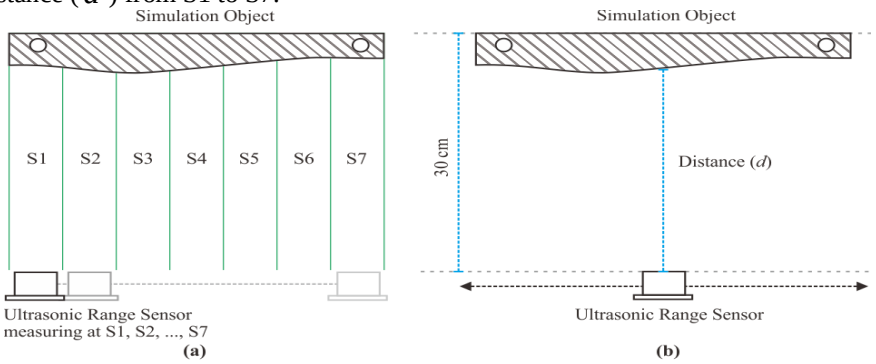

Figure 4. Measurement scheme using ultrasonic sensor; (a) Segmented measurement using ultrasonic sensor; (b) Sensor and object position

4. RESULTS AND ANALYSIS

After several experiments, a discussion about result of vein image processing, back-projection on flat and multi surface is provided. Image processing algorithm was tested directly to the skin in order to obtain the vein pattern and performing back-projection as the last process. However, to observe the back-projection performance directly to the human skin is difficult to do since a static position of object is required. Therefore, a various surface objects as shown in Figure 2 was used to test the performance of back-projection method.

4.1. Image Processing Result

The results of the image processing process in each step are shown in Figure 5. Veins image obtained by the camera was not seen clearly where the difference between veins and skin was not strong enough. The information on veins image contains only dark and bright areas thus the grayscale process needs to be done. In emphasizing the difference between veins and the skin, adaptive histogram equalization provides good results where the veins become slightly clearer.

In the segmentation stage, the vein pattern was able to be separated from the skin by using adaptive thresholding. However, there was also a segmented noise from the segmentation process. Morphology operation such as opening and closing was performed to remove the noise. Although the results were not significant, noise could be overcomed by the morphology process. Before being projected, a coloring process was applied to the results of morphology to avoid white lights.

Previous research with dual camera configurations requires a PC with a high-speed processor to perform back-projection [4]. Meanwhile in this study, with the configuration in **Error! Reference source not found.**.a, the whole process tooks between 65 ms. The computation time is relatively fast considering that the process was processed by a portable single board computer. The last process is to re-project the vein image onto the surface of the skin. The projection performance results will be discussed in the next section.

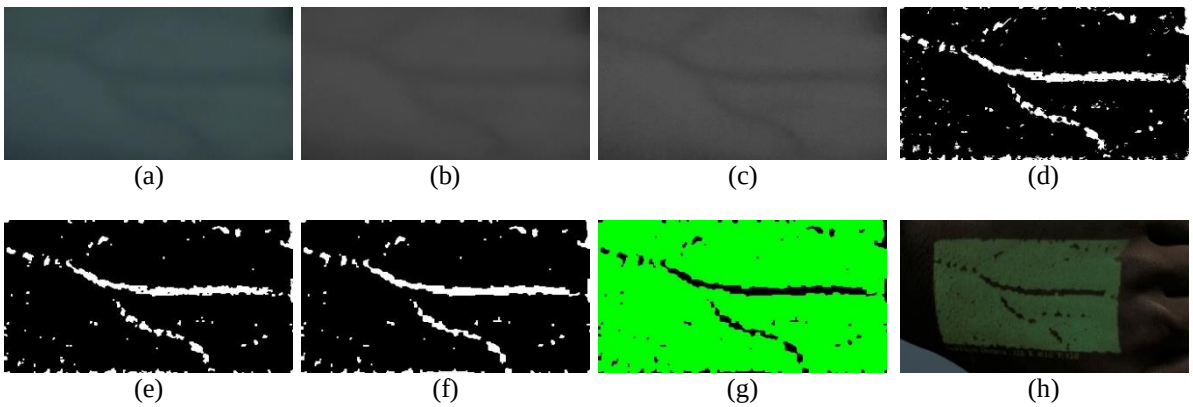

Figure 5. Image processing result (a) original image; (b) grayscale result; (c) adaptive histogram equalization result; (d) adaptive thresholding result; (e) morphology opening result; (f) morlphology closing result; (h) projected vein image result

4.2. Result of back-projection on flat surface

The test of back-projection at various distances with flat objects have excellent results. In this measurement, the position of the ultrasonic distance the sensor was kept perpendicular to the object even though the distance varies. From the results shown in Table 1, x locations have a maximum shift of 0.25 mm whereas for y locations have a maximum shift of 0.48 mm.

Table 1. Result of Measurement Using Flat Surface in Various Distance

Distance (cm)	20	25	30	35	40
x actual (pixel)	530	498	475	456	444
y actual (pizel)	-105	-46	-4	26	47
x measured (pixel)	530	497	475	456	444
y measured (pixel)	-107	-46	-6	25	47
x shift (mm)	0	0	0	0.25	0
y shift (mm)	0.3	0	0.48	0.25	0

4.3. Result of back-projection on various surface objects

Figure 6(a) shows how the projection shift is obtained. A vein vessel is simulated by blue lines and the projected veins have a yellow color. A projection shift occurred when yellow lines overlap the blue lines. Since the vein diameter for IV access (cephalic veins) is range from 1.5 to 6 mm [25], a simulated vein size was set to 3.75 mm (median value).

Figure 6(b) shows the projection shift that can still be tolerated. It can be seen that the unaccepted coverage area is covering less than 75% of vein vessel or maximum projection shift that can be tolerated is 0.93 mm. Coverage area less than 75% will cause the needle insertion shift to the edge of the vein vessel or missed because the reference point is the center of projected veins.

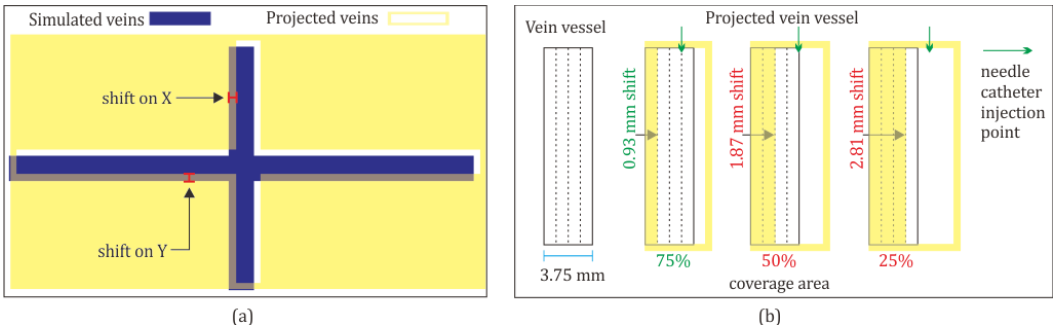

Figure 6. (a) Projection shift measurement; (b) Projection coverage area

Table 2 shows the results of projection shift on objects with multi-surface. From all objects, the most consistent projection shift occurred in each S1 and S7 where these segments are close to the edge of the object. The projection shifts on each S1 and S7 may occur because these segments are not fully covered by the transducer. By ignoring the error in S1 and S7, some segments that have projection shift exceeding 0.9 mm are in (C: 3,4,5), (D: 3), and (E: 6). This projection shifts occurred because the distance reading encountered a considerable error in these segments.

The most projection shift occurred in S1 and S7 because the location of these segments is close to the edge of the object. While in the other segments, a large projection shift probably occurs due to large rotation angles to the sensor or steep curvature. Meanwhile, the other segments have projection shift lower than 0.9 mm. There are a few segments that almost have projection shift close to zero. Segments (A: 3,4,5), (D: 4,6), (E: 3), (F: 2,3,4,5,6), (G: 3,4,5), (H: 3,5), and (I: 2,4,5,6) have projection shift lower than 0.2 mm. It can be seen that the segments with a small projection shift have a less curved surface or the rotation angle between object and sensor is close to perpendicular. However, even though (H:3,5) have a curved surface,

the projection shift is lower than 0.2 mm. It is possibly occurred because the ultrasonic distance sensor also covers the neighbor of these segments and unfortunately made the distance reading have less error.

Table 2. Result of Projection Shift Measurement in Millimeter

Object		S1	S2	S3	S4	S5	S6	S7
A	X	0.5	0.2	0.1	0.1	0.1	0.2	0.5
	Y	0.9	0.4	0.2	0.2	0.2	0.4	0.9
B	X	0.6	0.3	0.3	0.3	0.2	0.2	0.5
	Y	1.0	0.6	0.5	0.5	0.3	0.4	0.8
C	X	0.8	0.5	0.8	0.5	0.6	0.3	0.7
	Y	1.4	0.9	1.3	0.9	1.0	0.5	1.2
D	X	0.3	0.3	0.7	0.0	0.2	0.1	0.5
	Y	0.5	0.6	1.2	0.0	0.3	0.1	1.0
E	X	0.8	0.3	0.1	0.3	0.6	0.7	0.4
	Y	1.5	0.5	0.1	0.6	1.0	1.3	0.7
F	X	0.4	0.1	0.0	0.1	0.0	0.1	0.4
	Y	0.8	0.2	0.0	0.1	0.0	0.2	0.8
G	X	0.5	0.2	0.1	0.1	0.1	0.2	0.6
	Y	0.9	0.3	0.2	0.1	0.2	0.3	1.1
H	X	0.5	0.2	0.1	0.5	0.0	0.1	0.4
	Y	0.8	0.4	0.1	0.8	0.1	0.3	0.7
I	X	0.5	0.1	0.2	0.1	0.1	0.1	0.5
	Y	0.9	0.2	0.3	0.2	0.2	0.2	0.9
J	X	0.6	0.3	0.3	0.3	0.3	0.3	0.7
	Y	1.1	0.6	0.5	0.5	0.5	0.6	1.2

A test of the rotation angle between objects and sensors was conducted due to many projection shifts occur on the surface with a fairly high rotation angle. This test aims to know the characteristic of distance reading to the real distance in various rotation angle. Figure 3.b shows the measurement setup where there is a flat surface that can rotate from 10 to -10 degrees against the ultrasonic sensor. The distance between the object and the sensor was set at 30 cm. The measurement results with a 2-degree step are shown in Table 3. From these results, it can be seen that the sensor reading error was directly proportional to the rotation angle.

In this study, objects B, F, and G have convex profiles, while objects I and J have concave profiles. The other objects that were not mentioned above have various curvatures. Therefore, objects B, F, G, I, and J are easier to analyze by arranging several forming lines. In its implementation, each segment has a forming line with different angles toward the ultrasonic sensor as shown in Figure 7.

Table 3. Difference of Distance Reading to Real Distance in Flat Object Rotation

Rotation (deg)	Pos A (cm)	Pos B (cm)	Pos C (cm)	Rotation (deg)	Pos A (cm)	Pos B (cm)	Pos C (cm)
-10	1.16	1.00	1.05	0	0.00	0.00	0.00
-8	0.98	0.70	1.02	2	0.23	0.00	0.37
-6	0.81	0.40	0.89	4	0.76	0.20	0.54
-4	0.54	0.20	0.66	6	0.99	0.40	0.71
-2	0.27	0.10	0.13	8	1.12	0.80	0.89
0	0.00	0.00	0.00	10	1.15	1.00	1.16

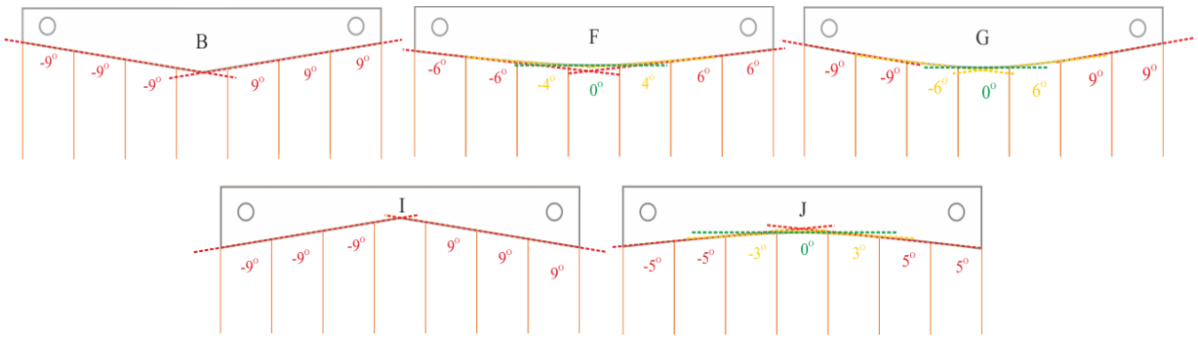

Figure 7. Multi angle forming line on each object

Based on the results of the formed straight line, an approach can be made with the results of flat surface rotation as shown in Table 3. From the 5 objects shown in Figure 7, the highest rotation of forming line is ±9 degrees. Objects B and J were formed with lines at the ±9 degrees rotation in each segment. Object F was formed with lines at ±6, ±4, and 0 degrees rotation. Object G was formed with lines at ±9, ±6, and 0 degrees rotation. Object I was formed with lines with ±5 and 0 degrees rotation.

Table 4 shows the results of distance measurements of object B, F, G, I, and J. Objects B and I have close errors and can be classified as objects with the highest error because both have the same forming angle of 9 degrees in each segment. Objects F and G also have almost the same shape. A higher error has occured in Object G because there was a forming line of ±9 degrees on S1, S2, S6, and S7. While object F in the same segment is formed by a line of ±6 degrees. Object I has a smaller error than other objects because the forming line has an angle of 5 and 0 degrees. However, in its implementation only S2 and S6 have errors smaller than others, while S3, S4, and S5 have errors that are almost similar to object G which is formed by a line of -6, 0, and 6 degrees in the same segment. This result has the same characteristic as the results in Table 3 even though the value is not the same. So far it can be concluded that increasing the rotation angle of an object against the distance sensor will increase errors in distance reading.

Table 4. Difference Between Real Distance and Measured Distance

	Difference between real distance and measured distance (cm)						
Object	S1	S2	S3	S4	S5	S6	S7
B	0.58	0.32	0.27	0.27	0.17	0.22	0.48
F	0.44	0.13	0	0.07	0	0.13	0.44
G	0.53	0.19	0.09	0.05	0.09	0.19	0.63
I	0.5	0.1	0.19	0.1	0.14	0.1	0.5
J	0.6	0.33	0.28	0.26	0.28	0.33	0.7

From this analysis, so far it could be known that increasing the angle of a segment towards the sensor will also increase the error of distance reading. Since the location of the projection depends on the distance reading, increasing the angle of a segment will increase the shift in back-projection. The profile of human skin generally resembles objects F and G. Therefore, applying this system to the skin may actually have a projection error like those objects. By knowing the characteristics of F and G, the location of the sensor must be at the midpoint (S3, S4, S5) to minimize projection errors in the actual plant.

5. CONCLUSION

The performance evaluation of the proposed system in this study was successfully carried out. By utilizing a single board computer, the whole computations for 1 frame were successfully carried out with a total time about 65 ms (15 fps). The use of ultrasonic sensor in the projection method has good results when measuring flat surface object with maximum projection shift of 0.48 mm. The test results on several samples with various surfaces have good results where the projection shifts below 0.9 mm reach 89% of 140 measurement points. Some large projection shift occurs because the distance sensor reading occurrences an error caused by the surface of the object that has a steep curvature or a large rotation angle to the sensor.

REFERENCES

[1] S. Juric and B. Zalik, "An innovative approach to near-infrared spectroscopy using a standard mobile device and its clinical application in the real-time visualization of peripheral veins," *BMC Med. Inform. Decis. Mak.*, vol. 14, no. 1, pp. 1–9, 2014.
[2] H. K. Al Ghozali, Setiawardhana, and R. Sigit, "Vein detection system using infrared camera," *2016 Int. Electron. Symp.*, pp. 122–127, 2016.
[3] A. Marcotti, M. B. Hidalgo, and L. Mathe, "Non-invasive vein detection method using infrared light," *IEEE Lat. Am. Trans.*, vol. 11, no. 1, pp. 263–267, 2013.
[4] D. Ai *et al.*, "Augmented reality based real-time subcutaneous vein imaging system," *Biomed. Opt. Express*, vol. 7, no. 7, p. 2565, 2016.
[5] I. P. Adi Surya Gunawan, R. Sigit, and A. I. Gunawan, "Vein Visualization System Using Camera and Projector Based on Distance Sensor," in *2018 International Electronics Symposium on Engineering Technology and Applications (IES-ETA)*, 2018, pp. 150–156.
[6] B. Mustapha, A. Zayegh, and R. K. Begg, "Ultrasonic and Infrared Sensors Performance in a Wireless Obstacle

Detection System," in *2013 1st International Conference on Artificial Intelligence, Modelling and Simulation*, 2013, pp. 487–492.
[7] T. Mohammad, "Using Ultrasonic and Infrared Sensors for Distance Measurement," *Int. J. Mech. Aerospace, Ind. Mechatron. Manuf. Eng.*, vol. 03, no. 03, pp. 267–272, 2009.
[8] A. Gontean, "Performance Evaluation of Ultrasonic Sensors Accuracy in Distance Measurement," in *2014 11th International Symposium on Electronics and Telecommunications (ISETC)*, 2014, pp. 1–4.
[9] S. Prahl, "Optical Arbsorption of Hemoglobin," 1999. [Online]. Available: https://omlc.org/spectra/hemoglobin/. [Accessed: 21-Jan-2018].
[10] G. J. Tserevelakis *et al.*, "Photoacoustic imaging reveals hidden underdrawings in paintings," *Sci. Rep.*, vol. 7, no. 1, pp. 1–11, 2017.
[11] A. A. Aziz and W. R. W. Ahmad, "Train obstacle detection system using Avr microcontroller and SR04 ultrasonic sensor," *Indones. J. Electr. Eng. Comput. Sci.*, vol. 9, no. 3, pp. 650–654, 2018.
[12] K. Huang, C. Chang, H. Chang, and C. Chang, "The image analysis of skin tissue irradiated with difference wavelengths of LED sources," in *2012 IEEE International Instrumentation and Measurement Technology Conference Proceedings*, 2012, pp. 1246–1250.
[13] W. Dong *et al.*, "Research on multi-spectral adaptive method for palm vein capturing based on image quality," *Proc. - 2017 32nd Youth Acad. Annu. Conf. Chinese Assoc. Autom. YAC 2017*, no. 31401285, pp. 1154–1157, 2017.
[14] F. Wang, A. Behrooz, M. Morris, and A. Adibi, "High-contrast subcutaneous vein detection and localization using multispectral imaging," *J. Biomed. Opt.*, vol. 18, no. 5, p. 050504, 2013.
[15] C. Pal, A. Chakrabarti, and R. Ghosh, "A Brief Survey of Recent Edge-Preserving Smoothing Algorithms on Digital Images," no. March, 2015.
[16] P. Liu, S. Di, J. Jin, and L. Bai, "Enhancement display of veins distribution based on binocular vision and image fusion technology," vol. 9268, p. 92681E, 2014.
[17] A. S. Aziz, R. Sigit, A. Basuki, and T. Hidayat, "Cardiac Motions Classification on Sequential PSAX Echocardiogram," *Indones. J. Electr. Eng. Comput. Sci.*, vol. 12, no. 3, pp. 1289–1296, 2018.
[18] O. C. Kurban, O. Niyaz, and T. Yildirim, "Neural network based wrist vein identification using ordinary camera," *Proc. 2016 Int. Symp. Innov. Intell. Syst. Appl. INISTA 2016*, 2016.
[19] D. Kim, Y. Kim, S. Yoon, and D. Lee, "Preliminary study for designing a novel vein-visualizing device," *Sensors (Switzerland)*, vol. 17, no. 2, 2017.
[20] A. Singh, S. C. P. Kumar, and B. G. Sudershan, "Non-Invasive Vein Detection using Infra-red Rays," vol. 5, no. 8, pp. 309–313, 2016.
[21] Z. Wu *et al.*, "A vein image enhancement algorithm for the multi-spectral illumination," *IST 2013 - 2013 IEEE Int. Conf. Imaging Syst. Tech. Proc.*, pp. 332–336, 2013.
[22] Q. Zhu, Z. Zhang, N. Liu, and H. Sun, "Near infrared hand vein image acquisition and ROI extraction algorithm," *Optik (Stuttg).*, vol. 126, no. 24, pp. 5682–5687, 2015.
[23] T. Ahmed *et al.*, "Real Time Injecting Device With Automated Robust Vein Detection Using Near Infrared Camera And Live Video," 2017.
[24] P. Popielski, R. Koprowski, and Z. Wróbel, "The matching method for veins images," *Comput. Med. Imaging Graph.*, 2017.
[25] R. Sharp *et al.*, "Measurement of Vein Diameter for Peripherally Inserted Central Catheter (PICC) Insertion: An Observational Study," *J. Infus. Nurs.*, vol. 38, no. 5, pp. 351–357, 2015.